JOURNAL OF AGRICULTURAL AND FOOD CHEMISTRY

Article

pubs.acs.org/JAFC

Metabolomics by Proton High-Resolution Magic-Angle-Spinning Nuclear Magnetic Resonance of Tomato Plants Treated with Two Secondary Metabolites Isolated from *Trichoderma*

Pierluigi Mazzei,[*,†] Francesco Vinale,[‡] Sheridan Lois Woo,[‡,§] Alberto Pascale,[§] Matteo Lorito,[‡,§] and Alessandro Piccolo[†,§]

[†]Centro Interdipartimentale per la Risonanza Magnetica Nucleare per l'Ambiente, l'Agro-Alimentare ed i Nuovi Materiali (CERMANU), Università di Napoli Federico II, Via Università 100, 80055 Portici, Città Metropolitana di Napoli, Italy

[‡]Istituto per la Protezione Sostenibile delle Piante, Consiglio Nazionale delle Ricerche (CNR), Via Università 133, 80055 Portici, Città Metropolitana di Napoli, Italy

[§]Dipartimento di Agraria, Università degli Studi di Napoli Federico II, Via Università 100, 80055 Portici, Città Metropolitana di Napoli, Italy

Supporting Information

ABSTRACT: *Trichoderma* fungi release 6-pentyl-2*H*-pyran-2-one (**1**) and harzianic acid (**2**) secondary metabolites to improve plant growth and health protection. We isolated metabolites **1** and **2** from *Trichoderma* strains, whose different concentrations were used to treat seeds of *Solanum lycopersicum*. The metabolic profile in the resulting 15 day old tomato leaves was studied by high-resolution magic-angle-spinning nuclear magnetic resonance (HRMAS NMR) spectroscopy directly on the whole samples without any preliminary extraction. Principal component analysis (PCA) of HRMAS NMR showed significantly enhanced acetylcholine and γ-aminobutyric acid (GABA) content accompanied by variable amount of amino acids in samples treated with both *Trichoderma* secondary metabolites. Seed germination rates, seedling fresh weight, and the metabolome of tomato leaves were also dependent upon doses of metabolites **1** and **2** treatments. HRMAS NMR spectroscopy was proven to represent a rapid and reliable technique for evaluating specific changes in the metabolome of plant leaves and calibrating the best concentration of bioactive compounds required to stimulate plant growth.

KEYWORDS: *6-pentyl-α-pyrone, harzianic acid, metabolomics, Trichoderma secondary metabolites, HRMAS NMR*

INTRODUCTION

Plant-growth-promoting microorganisms, such as fungi, have been naturally sustaining the agricultural production that allowed the human population to grow over millennia.[1] *Trichoderma* probably represents the most popular genera of fungi commercially available as a plant growth promoter and biological control agent for agricultural and industrial applications.[2,3] The principal attractiveness of *Trichoderma* consists in its efficient and diversified capability to perform antagonistic activities against various soil-borne phytopathogens[4] by means of mycoparasitism,[5] antibiosis,[6] and competition for nutrients in the rhizosphere.[7] Moreover, *Trichoderma* rhizosphere-competent strains exert direct effects on plants by stimulating plant defenses against biotic and abiotic damages as well as increasing their growth potential and nutrient uptake.[8,9] For instance, *Trichoderma harzianum* promotes the growth of tomato plants by influencing nutrients uptake with direct modulation of root development as well as through indirect mechanisms, such as mineral solubilization by acidification, redox, chelation, and hydrolysis reactions.[10]

Part of the beneficial functions enabled by the *Trichoderma*–plant interactions are activated and/or modulated by target molecules, which are released by the fungus and are prevalently ascribable to secondary metabolites.[2,11] Such compounds are biosynthesized from primary metabolites along specialized pathways and consist of relatively small molecules (generally <3 kDa), which may significantly vary according to individual fungal genera, species, or strains.[11,12] Although secondary metabolites are not directly involved in the primary metabolic fluxes, which are related to normal growth, development, or reproduction, they may play important roles in signaling interaction with other organisms.[1,13] *Trichoderma* strains produce and release a variety of compounds that induce resistance responses that prevent plant pathogenicity, such as systemic acquired resistance and rhizobacteria-induced systemic resistance.[2] Thus far, several potential biological activities have been attributed to *Trichoderma* secondary metabolites, including plant growth regulation, weed control effects, antibiotic, antiaging, antiplasmodial, cholesterol-lowering activity flavoring agents, immune suppression, and iron complexation.[3,6,14,15] It has been indicated that *T. harzianum* may significantly stimulate tomato growth via the production of an auxin-like phytohormone named harzianolide.[16] It is also noteworthy that organic acids released by *Trichoderma* strains,

Received: February 18, 2016
Revised: April 15, 2016
Accepted: April 18, 2016

DOI: 10.1021/acs.jafc.6b00801
J. Agric. Food Chem. XXXX, XXX, XXX−XXX

such as citric, oxalic, and tartaric acids, may chelate metals and solubilize potassium from K-containing minerals.

The secondary metabolites 6-pentyl-2*H*-pyran-2-one (alias 6-pentyl-α-pyrone, **1**) and harzianic acid (**2**) (Figure 1) isolated

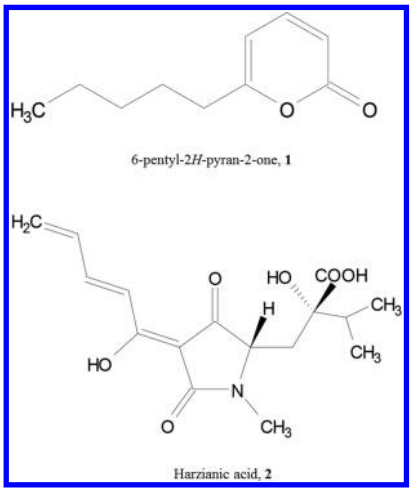

Figure 1. Structures of secondary metabolites 6-pentyl-2*H*-pyran-2-one (**1**) and harzianic acid (**2**) isolated from *T. atroviride* and *T. harzianum*, respectively.

from *Trichoderma* may significantly affect the physiology of several plants, including those in the Solanaceae family. The pyrone **1** is a volatile metabolite commonly purified from culture filtrates of different *Trichoderma* species (*Trichoderma viride*, *Trichoderma atroviride*, *T. harzianum*, and *Trichoderma koningii*) and associated with a number of beneficial properties, such as antipathogenic fungal activity,[17−19] plant growth promotion,[20] and production of coconut aroma.[21] The effectiveness of metabolite **1** in reducing the incidence of *Botrytis cinerea* and *Leptosphaeria maculans* on tomato and canola seedlings was confirmed in plants.[21] Interestingly, wheat seedling growth assays with metabolite **1** showed inhibitory effects at a high concentration and growth promotion at a low concentration. However, in foliar spray treatments on tomato, metabolite **1** at the 0.166 mg/L concentration produced vigorous growth and an extensive root system.[21]

Harzianic acid recently isolated from a *T. harzianum* strain[22] was shown to be a tetramic acid derivative and characterized by the presence of a pyrrolidinedione ring system. The metabolite **2** revealed *in vitro* antibiotic activity against *Pythium irregulare*, *Sclerotinia sclerotiorum*, and *Rhizoctonia solani*.[22,23] The application of metabolite **2** to canola seedlings at the concentrations of 100 and 10 μg/seed inhibited stem length, whereas the lower concentrations of 100, 10, and 1 ng/seed increased stem length by 42, 44, and 52% more than the control, respectively.[22] Moreover, it has been recently shown that metabolite **2** from *T. harzianum* may have a large binding affinity to essential metals, such as Fe^{3+}, thus potentially serving as a siderophore.[24] Despite the large body of literature on the effects of metabolites **1** and **2** on plants, limited information is yet available on the molecular mechanisms by which these secondary metabolites exert their bioactivity. Therefore, further investigations are required to identify not only the changes in metabolic profiles promoted by treatments with different concentrations of secondary metabolites but also the underlying biomolecular mechanisms in plants.[1]

Advanced analytical technologies are necessary to reach detailed molecular identification of plant metabolic profiles induced by treatments. In comparison to other techniques, nuclear magnetic resonance (NMR) spectroscopy achieves high throughput and simultaneous structural information on a wide range of metabolites with great analytical precision and accuracy. As a result of such advantages, NMR spectroscopy is an increasing choice in metabolomic studies and has proven to enable identification of treatment-dependent metabolic processes occurring in plants,[25−28] including those of tomato plants.[29−34] Moreover, the high-resolution magic-angle-spinning (HRMAS) technique enables a direct application of NMR spectroscopy to semi-solid samples, such as fresh plant leaves, and a rapid achievement of sample metabolic profiles.[35,36] The HRMAS NMR technique enables the acquisition of molecular fingerprinting of semi-solid samples with a similar resolution to that of classical liquid-state NMR techniques, thereby providing simultaneous information on polar and nonpolar components of plant tissues without the need for preliminary sample extractions.[37]

The aim of this work was thus to characterize the metabolome of tomato leaves treated with *Trichoderma* secondary metabolites **1** and **2** by ^{1}H HRMAS NMR spectroscopy and evaluate the metabolic changes brought about by different treatment rates.

MATERIALS AND METHODS

Fungal Material. The *Trichoderma* strains used were from the microbial collection of the Biological Control Laboratories of the Department of Agriculture, University of Naples Federico II. The strains *T. harzianum* M10 and *T. atroviride* P1 were maintained on potato dextrose agar (PDA) medium (HiMedia, Laboratories Mumbai, India) covered with sterilized mineral oil (Sigma-Aldrich, St. Louis, MO).

Isolation and Characterization of *Trichoderma* Secondary Metabolites. Six pentyl-α-pyrone (**1**) and harzianic acid (**2**) secondary metabolites were isolated by *T. harzianum* M10 and *T. atroviride* P1, respectively, as follows. The fungi were grown in 2.5 L of potato dextrose broth (PDB, Sigma-Aldrich, St. Louis, MO) stationary cultures at 25 °C in 5 L conical flasks inoculated with small pieces of the PDA cultures. After 30 days, the liquid cultures of each strain were filtered through No. 4 filter paper (Whatman, Brentford, U.K.) and exhaustively extracted with ethyl acetate (EtOAc, Sigma-Aldrich, St. Louis, MO). The separated organic fractions were first treated with $NaSO_4$ (Sigma-Aldrich) to remove water moisture and then dried by vacuum rotoevaporation at 35 °C.

The dried extract from the P1 culture was separated by flash column chromatography on 50 g of GF60 silica gel, 35−70 mesh (Merck, Darmstadt, Germany) as previously described,[21] whereas the residue from the M10 strain was first redissolved in CH_3Cl and then extracted by a 2 M NaOH solution that was subsequently added to 2 M HCl to precipitate the organic acids. The solid was recovered by filtering the solution through a 0.3 μm Buchner filter. The material retained on the filter was redissolved in EtOAc and dried by vacuum rotoevaporation at 35 °C. The dried residue was then subjected to RP-C18 column chromatography as previously reported.[12]

***In Vitro* Plant Growth Assay.** Tomato plants cv. "Roma" (*Solanum lycopersicum*) were grown *in vitro* to evaluate the influence exerted on the plant metabolome by *Trichoderma* secondary metabolites **1** and **2**. Tomato seeds were surface-sterilized with 1% NaClO for 10 min and extensively rinsed with sterile water. The seeds (20 per treatment) were germinated in Magenta boxes filled with 20 mL of half-strength Murashige and Skoog solution (MS Duchefa Biochemie, Haarlem, Netherlands) and 1% agar. The *Trichoderma* secondary metabolites were added to the medium in the boxes and stirred before the solidification of the agar. Starting from a 10 mM stock solution, secondary metabolites were diluted to reach the

DOI: 10.1021/acs.jafc.6b00801
J. Agric. Food Chem. XXXX, XXX, XXX−XXX

Table 1. Percentage (%) of Tomato Seed Germination Following Treatment with Different Concentrations of 6-Pentyl-2*H*-pyran-2-one (1) and Harzianic Acid (2) Metabolites[a]

treatment	24 h	SD	48 h	SD	72 h	SD	96 h	SD
control	0.0 a	0	16.7 a	3.9	72.2 a	7.9	100.0 a	0
$\mathbf{2}_{max}$	0.0 a	0	88.9 b	3.9	94.4 b	3.9	100.0 a	0
$\mathbf{2}_{int}$	0.0 a	0	72.2 c	7.9	100.0 c	0.0	100.0 a	0
$\mathbf{2}_{min}$	0.0 a	0	27.8 ad	11.8	72.2 ad	11.8	100.0 a	0
$\mathbf{1}_{max}$	0.0 a	0	44.4 e	7.9	88.9 e	7.9	100.0 a	0
$\mathbf{1}_{min}$	0.0 a	0	11.1 g	0.0	61.1 g	11.8	100.0 a	0

[a]Values are means of three replicates (20 seeds per pot). SD = Standard Deviation. Values with the same letter do not differ significantly ($p < 0.05$). Control, min, int, and max indicate secondary metabolite concentrations of 0, 0.1, 1, and 10 μM, respectively.

concentrations of 10 μM ($\mathbf{1}_{max}$ and $\mathbf{2}_{max}$) and 0.1 μM ($\mathbf{1}_{min}$ and $\mathbf{2}_{min}$). Only in the case of harzianic acid, it was used at an intermediate concentration corresponding to 1 μM ($\mathbf{2}_{int}$). The total set of samples also included control seeds, which were not exposed to *Trichoderma* secondary metabolites. To evaluate the direct influence exerted on seeds by *Trichoderma* secondary metabolites, the germination rate was measured by quantitating the percent of germinated seeds as a function of time. The significance of the germination rate was assessed by one-way analysis of variance (ANOVA; Tukey's test).

Each treatment consisted of three replicates and was repeated twice for a total of six replicates per treatment. Plants were grown in a growth chamber at 25 °C (16 h photoperiod) and harvested 15 days after seeding. Plants were harvested randomly from each replicate to obtain five different pools containing leaves from three plants. After harvesting, the whole plants were weighed and stored at −80 °C until NMR analysis.

NMR Experiments. Each sample for NMR analysis was prepared by cutting in small pieces about 15 ± 2 mg (fresh weight) of tomato leaves from the same treatment. This plant material was packed into a HRMAS NMR 4 mm zirconia rotor fitted with a perforated Teflon insert, soaked with approximately 15 μL of 99.8% D_2O (Armar Chemicals, Döttingen, Switzerland), and sealed with a Kel-F cap (Rototech-Spintech GmbH, Griesheim, Germany). The rotor was spun at a rate of 5000 ± 1 Hz. All NMR experiments were conducted at 25 °C on a 400 MHz Avance magnet (Bruker Biospin, Rheinstetten, Germany), equipped with a $^1H-^{13}C$ HRMAS probe working at ^{13}C and ^1H frequencies of 101.5 and 400.13 MHz, respectively. A Carr−Purcel−Meiboom−Gill (CPMG) NMR pulse sequence was used to acquire ^1H spectra of tomato leaves. This sequence was preferred to the conventional ^1H acquisition because it consists of a T_2 filter enabling the selective suppression of those compounds characterized by a short spin−spin relaxation time. The experiments were acquired by setting 2 s of recycle delay, a 90° pulse length ranging within 5.2 and 6.4 μs, 16 384 points, a spectral width of 16 ppm (6410.3 Hz), and 256 scans. In particular, the CPMG pulse sequence, which is based on a spin−echo method, was performed by applying a total spin−spin relaxation delay ($2n\tau$) of 320 ms composed by single optimal echo times (τ) of two ms. The signal of residual water was suppressed by applying the on-resonance presaturation during thermal equilibrium delay.

Structural identification of compounds detected in tomato leaves was assessed by two-dimensional (2D) NMR experiments, such as homonuclear $^1H-^1H$ correlation spectroscopy (COSY), total correlation spectroscopy (TOCSY), and *J*-RES, as well as heteronuclear $^1H-^{13}C$ heteronuclear single-quantum correlation (HSQC) and heteronuclear multiple-bond correlation (HMBC). All 2D experiments were acquired with a spectral width of 16 (6410.3 Hz) and 300 (30 186.8 Hz) ppm for ^1H and ^{13}C nuclei, respectively, and a time domain of 2048 points (F2) and 256 experiments (F1). Homonuclear 2D spectra were based on 16 dummy scans and 64 total transients. Additionally, a mixing time of 80 ms and a trim pulse length of 2500 ms were set for the TOCSY experiment. HSQC and HMBC heteronuclear experiments were acquired with 16 dummy scans, 80 total transients, and 0.5 μs of trim pulse length. The experiments were optimized by considering 145 and 6.5 Hz as the optimal $^1H-^{13}C$ short- and long-range *J* couplings, respectively. Spectra were processed using both Bruker Topspin software (version 2.1, BrukerBiospin, Rheinstetten, Germany) and MNOVA software (version 9.0, Mestrelab Research, Santiago de Compostela, Spain). Phase and baseline corrections were applied to all mono- and bidimensional spectra. Neither zero filling or apodization were necessary during the Fourier transformation of free induction decays. ^1H and ^{13}C axes were calibrated by associating the center of the β-CH_2 glutamine signal to 2.14 and 27.3 ppm, respectively.[29,32]

Multivariate Analysis. The region ranging from 0.1 to 9.22 ppm in ^1H CPMG NMR spectra was equally divided into 228 segments (each single bucket width corresponded to 0.04 ppm). Except for the region of the baseline distortion as a result of water suppression (4.9−4.66 ppm), all of these segments were integrated. Integration produced two data matrixes composed by 222 variables for 18 observations (6 replicates for 3 treatments) and 24 observations (6 replicates for 4 treatments) for the treatments **1** and **2**, respectively. Data were normalized by dividing each segment area by the sum of all signal areas and Pareto-scaled prior to performing principal component analysis (PCA).[38,39] The ANOVA test was applied to evaluate the significance (Tukey's test, confidence level of >95%) by which the most relevant variables differentiated the applied treatments. Statistical data elaboration was achieved by the XLStat software (version 2012, Addinsoft, Paris, France).

RESULTS AND DISCUSSION

Effect of Metabolites 1 and 2 on Seed Germination Rate and Seedling Growth. The influence on seed germination rates by the two *Trichoderma* secondary metabolites was assessed by incubating tomato seeds with different concentrations of metabolites **1** and **2**. The germination rate was quantitated for all treated seeds by assuming that germination occurred when the radicle protruded through the seed coat. The germination rate approached 100% within 96 h after seeding in all cases. Both *Trichoderma* secondary metabolites accelerated the germination rate, except for metabolite **1** at 0.1 μM concentration ($\mathbf{1}_{min}$) (Table 1). In fact, the treatment **2** promoted germination as soon as 24 h after seeding but depending upon the treatment rate, being about 5.3 times greater than the control for the $\mathbf{2}_{max}$ (88.9 versus 16.7%), while, for the intermediate concentration ($\mathbf{2}_{int}$), 100% germination was reached after 72 h. The positive effect exerted by metabolite **2** as germination promoter is in agreement with previous findings.[12] In the case of metabolite **1**, the treatment with $\mathbf{1}_{max}$ promoted seed germination but to a lower extent than for $\mathbf{2}_{max}$, whereas the $\mathbf{1}_{min}$ treatment even induced a slight inhibition within 72 h after seeding. Interestingly, this apparent inhibition shown by $\mathbf{1}_{min}$ is in agreement with previous reports on reduced germination rates for lettuce seeds incubated with metabolite **1** vapors.[20]

As shown in Figure 2, the *in vitro* plant growth promotion assay demonstrated that *Trichoderma* spp. secondary metabolites exerted an effect also on the seedling fresh weight.

DOI: 10.1021/acs.jafc.6b00801
J. Agric. Food Chem. XXXX, XXX, XXX−XXX

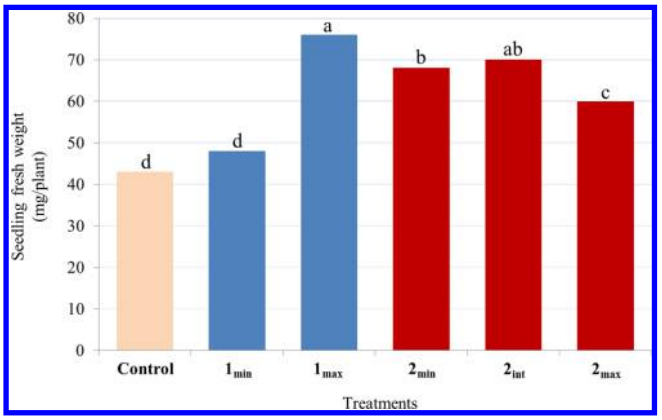

Figure 2. *In vitro* growth promotion assay of tomato seedlings treated with the secondary metabolites **1** and **2** at different concentrations and harvested 15 days after seeding. Values with the same letter do not differ significantly (p value < 0.05).

Treatment with metabolite **1** produced a dose-dependent effect directly proportional to the applied concentration with a weight increase of 76% ($\mathbf{1}_{max}$) and 13% ($\mathbf{1}_{min}$), as compared to the control. However, the variation induced in fresh weight by $\mathbf{1}_{min}$ was not significantly different from the control (p value $\leq$ 0.05). In comparison to the control, plants treated with $\mathbf{2}_{min}$, $\mathbf{2}_{int}$, and $\mathbf{2}_{max}$ showed a weight increase of 59, 65, and 39%, respectively, even though $\mathbf{2}_{int}$ and $\mathbf{2}_{max}$ did not statistically differ (p value $\leq$ 0.05). In agreement with the results on the seed germination rate, both secondary metabolites promoted seedling growth and, on the whole, the largest effects were caused by $\mathbf{1}_{max}$ and $\mathbf{2}_{int}$.

Metabolic Profiling of Tomato Leaves and Interpretation of NMR Spectra. The full ^{1}H CPMG NMR spectrum acquired for a representative sample of control tomato leaves is shown in Figure 3. Even though resolution for "semi-solid"

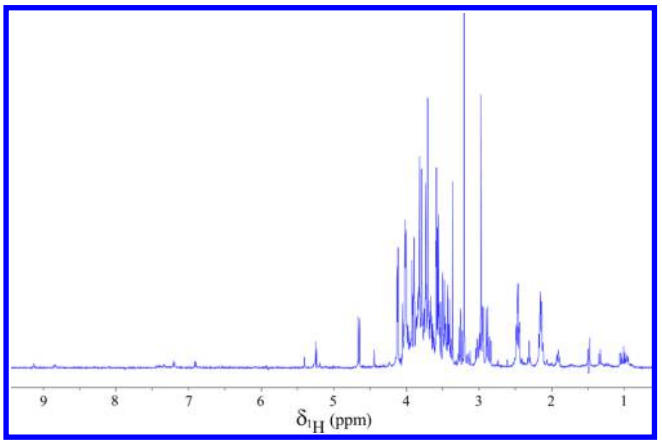

Figure 3. ^{1}H HRMAS CPMG NMR full spectrum of control tomato leaves acquired at a spin rate of 5 kHz.

samples may be relevantly improved by increasing the rotor spin rate,[35,40] it is known that an excessively fast rotation may force sample degradation and affect the analysis reliability. We thus adopted a moderate 5 kHz rotor spin rate that resulted as the best compromise to attain an overall resolution comparable to that of the solution state. The CPMG NMR pulse sequence enabled the selective suppression of proton signals for components with a short spin−spin relaxation time and characterized by typical broad peaks (i.e., relatively large molecules, including lipids and proteins). Consequently, the signal resolution was much improved, thereby facilitating compound assignments and their quantitative determination.

The CPMG NMR regions, (A) 0.8−3.3 ppm, (B) 3.34−4.27 ppm, and (C) 4.4−9.25 ppm, were magnified and shown in Figure 4. The assignment of main signals to specific compounds

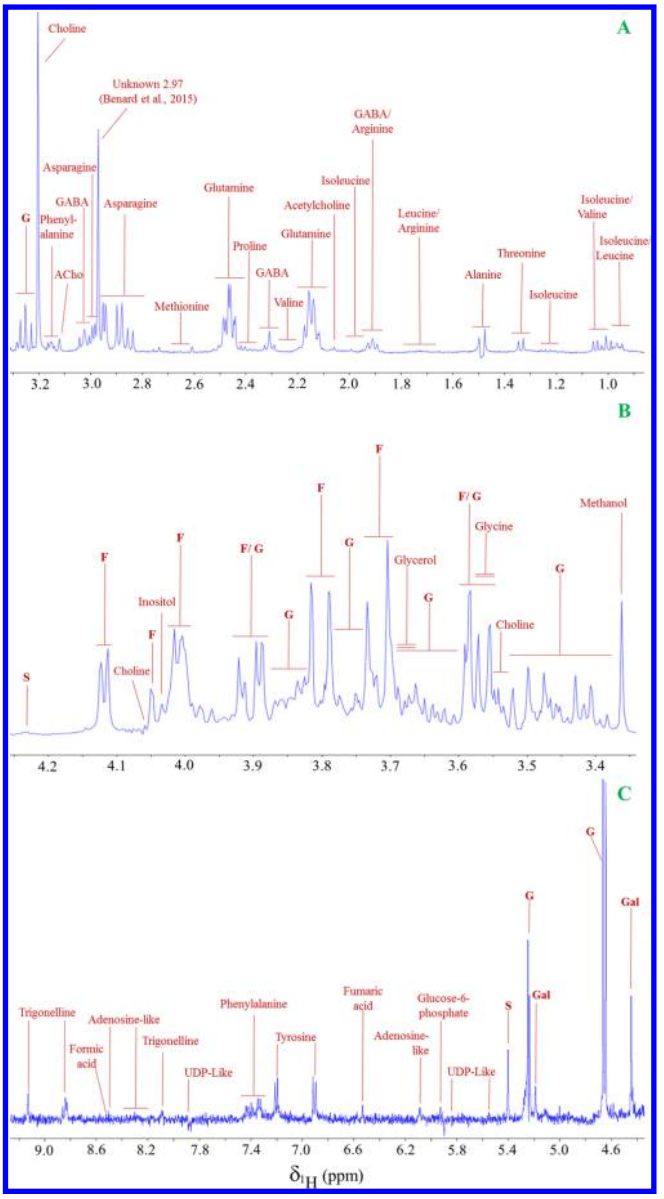

Figure 4. ^{1}H HRMAS CPMG NMR spectrum of control tomato leaves acquired at a spin rate of 5 kHz. Three spectral regions are shown: (A) 0.8−3.3 ppm, (B) 3.34−4.27 ppm, and (C) 4.4−9.25 ppm. The labels refer to assignment of the most intense signals detected in all treatments (F, fructose; G, glucose; Gal, galactose; S, sucrose; ACho, acetylcholine; GABA, γ-aminobutyric acid; and UDP, uridine diphosphate).

was made on the basis of homo- and heteronuclear 2D spectra and supported by previously described NMR attributions.[29−34] In particular, the 2D ^{1}H−^{13}C HSQC spectra, which reveals the short-range ($^1J_{CH}$) correlations between proton and carbon signals, confirmed resonance attributions by resolving the overlapped proton peaks through the second dimension (Figure 5). NMR spectra revealed that the most abundant

DOI: 10.1021/acs.jafc.6b00801
J. Agric. Food Chem. XXXX, XXX, XXX−XXX

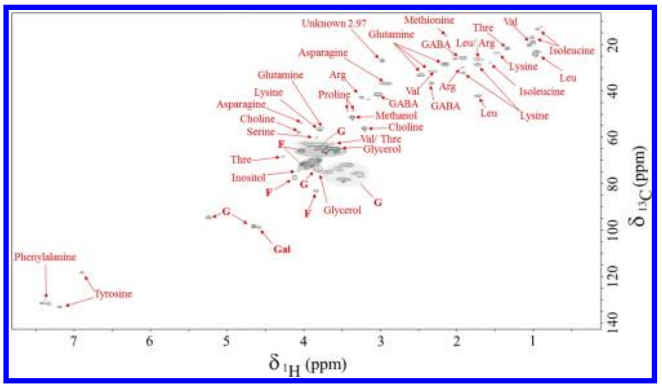

Figure 5. $^{1}H-^{13}C$ HSQC NMR spectrum of control tomato leaves optimized for a short-range J_{CH} coupling of 145 Hz. The labels refer to assignment of the most intense signals detected in all treatments (F, fructose; G, glucose; Gal, galactose; S, sucrose; GABA, γ-aminobutyric acid; Leu, leucine; Arg, arginine; Val, valine; and Thre, threonine). The ellipsoid regions circumscribe the dense cluster of F (dark gray) or G (light gray) signals.

molecules in leaves were carbohydrates, free amino acids, alcohols, and several organic acids (Figures 4 and 5), prevalently related to the primary metabolome of tomato plants. The ^{1}H spectra invariably showed a relatively intense δ ^{1}H singlet at 2.97 ppm (correlated to a δ ^{13}C at 27.2 ppm in 2D spectra) (Figures 4 and 5) that was impossible to assign ("unknown 2.97"), as also previously reported.[34] In comparison to control samples, both secondary metabolite treatments failed to reveal any new signal directly related to a specific treatment or at least any signal at a concentration compatible with the instrumental detection limit, whereas the relative concentration of several signals in spectra varied according to specific metabolite treatments. This result is in line with the different germination rates and the plant growth promotion data found with secondary metabolite additions (Table 1 and Figure 2) and suggests a treatment-dependent modulation in tomato metabolism.

Effect of 6-Pentyl-2*H*-pyran-2-one (1) on the Tomato Leaves Metabolome. Data from ^{1}H CPMG spectra were interpreted by multivariate PCA that greatly facilitated the evaluation of the very dense data matrices obtained from integration of signal regions. In fact, PCA is an unsupervised pattern-recognition technique that enables the efficient exploration of intrinsic variations within different sample classes.[38,39] PCA offers the practical advantage to explore in a single output (referred to as score plot) the metabolomic response induced in the whole set of samples by a large number of variables.[41,42] The PCA score plot in Figure 6A highlights the spectral behavior of samples treated with the lowest and highest concentrations of the metabolite **1**, with respect to that of the control. The distant spread among sample classes suggests that treatment **1** systematically affected the metabolome of tomato leaves (Figure 6A). On the other hand, the fact that replicates from the same treatment were projected relatively close to each other indicated good reproducibility for HRMAS spectra (Figure 6A). In particular, the PCA score plot combining the first and second principal components (58% of total explained variance) differentiated neatly the control from $\mathbf{1}_{min}$ samples along the PC1. As revealed by the related loading plot (Figure S1A of the Supporting Information), the $\mathbf{1}_{min}$ treatment produced a significantly larger amount of GABA, acetylcholine, and several amino acids, such as tyrosine, valine, glutamine,

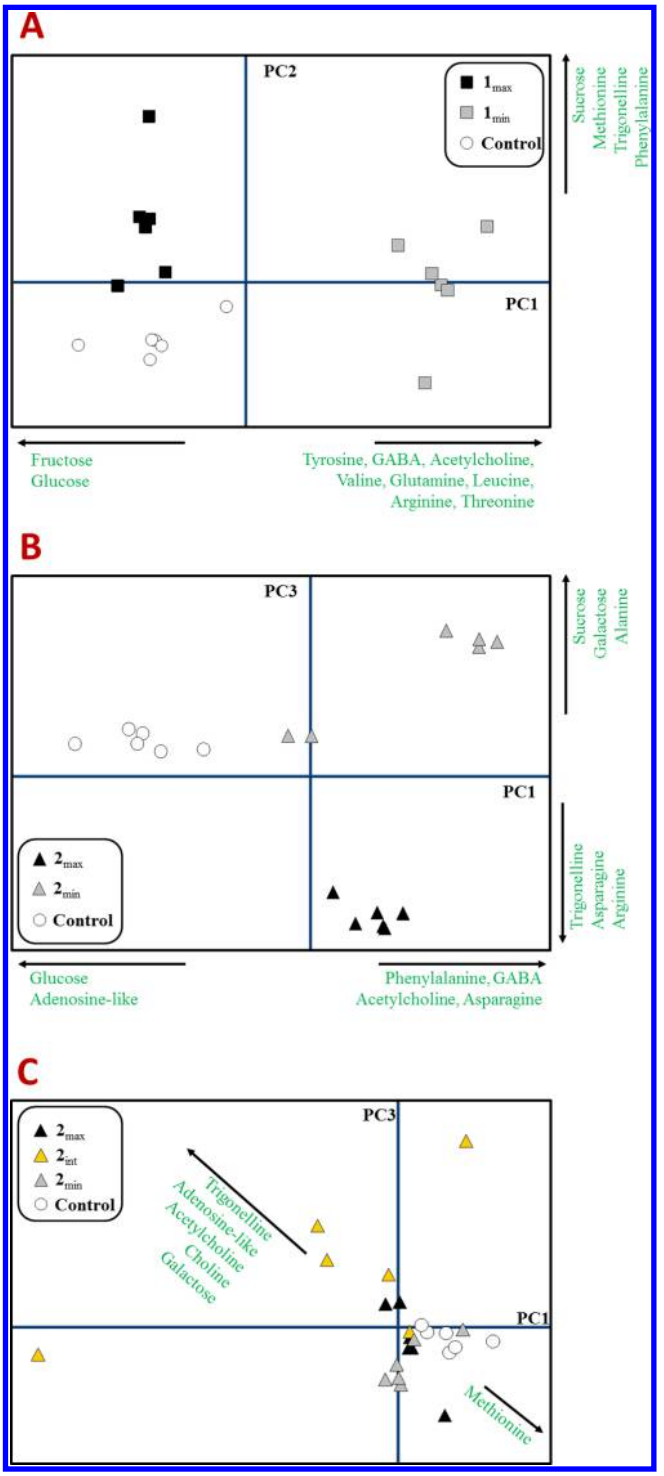

Figure 6. PCA score plots based on ^{1}H HRMAS CPMG spectra of leaves of tomato plants treated (A) with an increasing concentration of the metabolite **1** isolated from *T. atroviride* (control, $\mathbf{1}_{min}$, and $\mathbf{1}_{max}$) or with an increasing concentration of the metabolite **2** isolated from *T. harzianum* either (B) without (control, $\mathbf{2}_{min}$, and $\mathbf{2}_{max}$) or (C) including (control, $\mathbf{2}_{min}$, $\mathbf{2}_{int}$, and $\mathbf{2}_{max}$) the intermediate concentration of metabolite **2**. The name and direction of most significant loading vectors involved in the differentiation among treatments are reported.

leucine, arginine, and threonine, and a lower amount of glucose and fructose. Conversely, samples treated with $\mathbf{1}_{max}$ were vertically differentiated from control samples along the PC2 as

DOI: 10.1021/acs.jafc.6b00801
J. Agric. Food Chem. XXXX, XXX, XXX−XXX

a result of their larger amount of methionine, trigonelline, phenylalanine, and sucrose.

Direct or indirect beneficial effects on plants are commonly attributed to an excess of GABA and acetylcholine metabolites in plant cells.[43−45] Acetylcholine seems to mediate various physiological processes, including water balance, cell swelling, stomatal movement, root−shoot signal transduction, and cell elongation,[44] while GABA is reported to be involved in regulation of cytosolic pH and protection against oxidative stress.[45] The larger amount of fructose and glucose in control and $\mathbf{1}_{max}$ plants indicates a substantial accumulation of sugars in plant tissues and excess of monosaccharides in the vacuole.[46] The larger content of free amino acids found in $\mathbf{1}_{min}$ (Figure 6A) may indicate a limited biosynthesis of proteins resulting from possible stress conditions (i.e., lower nitrogen uptake). This is in agreement with the slight inhibition observed during germination under this secondary metabolite treatment (Table 1).

The $\mathbf{1}_{max}$ treatment produced a significantly larger content of trigonelline, phenylalanine, methionine, and sucrose than the control (Figure 6A). Methionine is a component of methionyl tRNA that is required to start protein synthesis as well as a direct precursor of *S*-adenosyl-methionine, the main biological methyl donor in many transmethylation reactions.[47] Sucrose was largely abundant in samples treated with $\mathbf{1}_{max}$, probably because this *Trichoderma* metabolite induced a more efficient photosynthetic process than the control. However, the fact that both glucose and fructose levels were very similar in both $\mathbf{1}_{max}$ and control samples, indicated the absence of monosaccharide catabolism during plant growth and excluded any induced inhibition of invertase enzymes. In the case of phenylalanine, its abundance is reported to enable massive enhancement of carbon flux following an increased demand for phenylpropanoid-derived metabolites, which have diverse physiological functions, including cell wall strengthening, plant defense, pigmentation, ultraviolet (UV) protection, and chemical signaling.[48,49] The presence of trigonelline, an alkaloid deriving from nicotinamide, is related to a number of processes occurring in plants, such as cell cycle regulation, nictinasty in leaves, osmoregulation for salt stress, and promotion of plant response to UV and oxidative stress.[50]

Effect of Harzianic Acid (2) on Tomato Leaves Metabolome. The PCA score plot obtained for samples treated with the smallest and largest concentrations of metabolite **2** is shown in Figure 6B. The neat separation between different treated samples (Figure 6B) suggests that treatment with the metabolite **2** elicited a specific and dose-dependent response in the tomato metabolome. In fact, the score plot (PC1 versus PC3, with a total explained variance of 36.6%) neatly differentiated control from samples $\mathbf{2}_{min}$ and $\mathbf{2}_{max}$. In comparison to metabolite **2**-treated samples, control plants were negatively correlated to PC1 because of their larger content of glucose and adenosine-like material, accompanied by a lower amount of GABA, acetylcholine, asparagine, and phenylalanine (Figure 6B and Figure S1B of the Supporting Information). Moreover, the fact that also the centroid position of the $\mathbf{2}_{min}$ group was distant from that of $\mathbf{2}_{max}$ suggests that all variables explained by PC1 not only differentiated control from both samples **2** but also $\mathbf{2}_{max}$ from $\mathbf{2}_{min}$ samples, even though at a lower semi-quantitative extent (Figure 6B). Moreover, a clear differentiation between samples treated with harzianic acid was also shown along PC3 and was due to both larger amounts of sucrose, galactose, and alanine and smaller contents of trigonelline, asparagine, and arginine in $\mathbf{2}_{min}$ (Figure 6B). On the other hand, the fact that control samples contained more glucose and even more amino acids than plants treated with harzianic acid (especially for $\mathbf{2}_{max}$ samples) indicated the amino acid biosynthesis was stimulated in the latter samples as already observed for treatment **1**. In particular, $\mathbf{2}_{max}$ samples were positioned in the fourth quadrant of the PCA score plot (Figure 6B) that was associated with the large content of phenylalanine, asparagine, and arginine. This response may be explained by a more pronounced biosynthesis of amino acids in harzianic-acid-treated samples. However, control samples also showed an excess of adenosine-like compounds. Unfortunately, the analytical lack of determination of the specific structure of this compound class prevented an understanding of their potential role in the plant. Interestingly, as already observed for $\mathbf{1}_{min}$ treatment, both treatments **2** increased the content of acetylcholine and GABA, whose accumulation in plant cells is considered beneficial to plants.[43−45]

The metabolites responsible for the differentiation between $\mathbf{2}_{min}$ and $\mathbf{2}_{max}$ along PC3 (Figure 6B) not only confirmed the occurrence of specific metabolic response in tomato plants but also underlined the importance of the dose of treatment in plant growth promotion. In this view, an intermediate dose ($\mathbf{2}_{int}$) was considered for treatment **2** as a result of a most effective hastening of seed germination within 48 h after seeding (Table 1). Figure 6C displays the PCA score plot of control samples and all other samples treated with harzianic acid. Interestingly, the combination of the first and third principal component revealed that $\mathbf{2}_{int}$ differed considerably from samples treated with the other two concentrations of metabolite **2** while concomitantly highlighted which metabolite variables were mostly responsible for the differentiation. In fact, the loading vectors for $\mathbf{2}_{int}$ samples were separated along a diagonal direction as a result of their relatively larger amounts of trigonelline, adenosine-like compounds, acetylcholine, choline, and galactose as well as lower amount of methionine (Figure 6C and Figure S1C of the Supporting Information).

Our findings indicate that HRMAS NMR spectroscopy allows for a rapid and accurate determination of the main molecular constituents of the tomato leaves metabolome by a direct evaluation of fresh samples, without any sample extraction. In addition, this work showed that the secondary metabolites **1** and **2** isolated from *Trichoderma* spp. are capable of affecting the composition of tomato leaves metabolome as a function of treatment dose. In fact, ^{1}H CPMG-edited spectra obtained by HRMAS NMR showed changes in sample metabolites that enabled development of PCA plots indicating significant differences among plant treatments and consequent inference on the involved specific metabolic processes.

Although a direct effect of these *Trichoderma* secondary metabolites on plant physiology had already been described, we enlarged the existing limited information by providing data on the related variations of the tomato leaves metabolome. It is expected that increased molecular knowledge on the mechanisms involved in plant interactions with the secondary metabolites applied here may be useful to develop new biofertilizers and/or biopesticides based on *Trichoderma* extracts.

■ ASSOCIATED CONTENT

Supporting Information

The Supporting Information is available free of charge on the ACS Publications website at DOI: 10.1021/acs.jafc.6b00801.

DOI: 10.1021/acs.jafc.6b00801
J. Agric. Food Chem. XXXX, XXX, XXX−XXX

Loading vectors related to PCA score plots shown in Figure 6 (Figure S1) (PDF)

AUTHOR INFORMATION

Corresponding Author

*Telephone: +39-0812539448. Fax: +39-0812539186. E-mail: pierluigi.mazzei@unina.it.

Funding

This work was supported by the Italian Ministry of Education, University and Research (MIUR), Programma Operativo Nazionale Ricerca & Competitivitá 2007−2013 (PON R&C 2007−2013) [Linfa PON03PE_00026_1 Marea PON03PE_00106, GenoPOM-pro PON02_00395_3082360, and SIcurezza e innovazione teCnologica Utile alla salvaguardia e valorizzazione dei prodotti tipici di oRigine Animale (SICURA)].

Notes

The authors declare no competing financial interest.

ABBREVIATIONS USED

HRMAS, high-resolution magic-angle-spinning; CPMG, Carr−Purcel−Meiboom−Gill; HSQC, heteronuclear single-quantum correlation

REFERENCES

(1) Lorito, M.; Woo, S. L.; Harman, G. E.; Monte, E. Translational research on *Trichoderma*: From 'Omics to the field. *Annu. Rev. Phytopathol.* **2010**, *48*, 395−417.

(2) Harman, G. E.; Howell, C. R.; Viterbo, A.; Chet, I.; Lorito, M. *Trichoderma* species − opportunistic, avirulent plant symbionts. *Nat. Rev. Microbiol.* **2004**, *2*, 43−56.

(3) Keswani, C.; Mishra, S.; Sarma, B. K.; Singh, S. P.; Singh, H. B. Unraveling the efficient applications of secondary metabolites of various *Trichoderma* spp. *Appl. Microbiol. Biotechnol.* **2014**, *98*, 533−544.

(4) Singh, B. N.; Singh, A.; Singh, S. P.; Singh, H. B. *Trichoderma harzianum*−mediated reprogramming of oxidative stress response in root apoplast of sunflower enhances defence against *Rhizoctonia solani*. *Eur. J. Plant Pathol.* **2011**, *131*, 121−134.

(5) Woo, S. L.; Lorito, M. Exploiting the interactions between fungal antagonists, pathogens and the plant for biocontrol. In *Novel Biotechnologies for Biocontrol Agent Enhancement and Management*; Vurro, M., Gressel, J., Eds.; Springer: Dordrecht, Netherlands, 2007; pp 107−130, DOI: 10.1007/978-1-4020-5799-1_6.

(6) Sivasithamparam, K.; Ghisalberti, E. L. Secondary metabolism in *Trichoderma* and *Gliocladium*. In *Trichoderma and Glioclaudium*; Kubicek, C. P., Harman, G. E., Eds.; Taylor & Francis: London, U.K., 1998; Vol *1*, pp 139−205.

(7) Benitez, T.; Rincon, A. M.; Limon, M. C.; Codon, A. C. Biocontrol mechanisms of *Trichoderma* strains. *Int. Microbiol.* **2004**, *7*, 249−260.

(8) Harman, G. E.; Chet, I.; Baker, R. *Trichoderma hamatum* effects on seed and seedling disease induced in radish and pea by *Pythium* spp. or *Rhizoctonia solani*. *Phytopathology* **1980**, *70*, 1167−1172.

(9) Shoresh, M.; Harman, G. E.; Mastouri, F. Induced systemic resistance and plant responses to fungal biocontrol agents. *Annu. Rev. Phytopathol.* **2010**, *48*, 21−43.

(10) Li, R. X.; Cai, F.; Pang, G.; Shen, Q. R.; Li, R.; Chen, W. Solubilisation of phosphate and micronutrients by *Trichoderma harzianum* and its relationship with the promotion of tomato plant growth. *PLoS One* **2015**, *10*, e0130081.

(11) Hanson, J. R.; *Natural Products: The Secondary Metabolites*; Abel, E. W., Ed.; Royal Society of Chemistry: Cambridge, U.K., 2003; DOI: 10.1039/9781847551535.

(12) Vinale, F.; Manganiello, G.; Nigro, M.; Mazzei, P.; Piccolo, A.; Pascale, A.; Ruocco, M.; Marra, R.; Lombardi, N.; Lanzuise, S.; Varlese, R.; Cavallo, P.; Lorito, M.; Woo, S. A novel fungal metabolite with beneficial properties for agricultural applications. *Molecules* **2014**, *19*, 9760−9772.

(13) Osbourn, A. Secondary metabolic gene clusters: Evolutionary toolkits for chemical innovation. *Trends Genet.* **2010**, *26*, 449−457.

(14) Vinale, F.; Girona, I. A.; Nigro, M.; Mazzei, P.; Piccolo, A.; Ruocco, M.; Woo, S. L.; Rosa, D. R.; Herrera, C. L.; Lorito, M. Cerinolactone, a hydroxy-lactone derivative from *Trichoderma cerinum*. *J. Nat. Prod.* **2012**, *75*, 103−106.

(15) Haas, H.; Eisendle, M.; Turgeon, B. G. Siderophores in fungal physiology and virulence. *Annu. Rev. Phytopathol.* **2008**, *46*, 149−187.

(16) Cai, F.; Yu, G.; Wang, P.; Wei, Z.; Fu, L.; Shen, Q.; Chen, W. Harzianolide, a novel plant growth regulator and systemic resistance elicitor from *Trichoderma harzianum*. *Plant Physiol. Biochem.* **2013**, *73*, 106−113.

(17) Claydon, N.; Allan, M.; Hanson, J. R.; Avent, A. G. Antifungal alkyl pyrones of *Trichoderma Harzianum*. *Trans. Br. Mycol. Soc.* **1987**, *88*, 503−513.

(18) Scarselletti, R.; Faull, J. L. *In Vitro* activity of 6-pentyl-a-pyrone, a metabolite of *Trichoderma harzianum*, in the inhibition of *Rhizoctonia solani* and *Fusarium oxysporum f.* sp. *Lycopersici*. *Mycol. Res.* **1994**, *98*, 1207−09.

(19) Worasatit, N.; Sivasithamparam, K.; Ghisalberti, E. L.; Rowland, C. Variation in pyrone production, pectic enzymes and control of rhizoctonia root rot of wheat among single-spore isolates of Trichoderma koningii. *Mycol. Res.* **1994**, *98*, 1357−63.

(20) Parker, R. S.; Cutler, H. G.; Jacyno, J. M.; Hill, R. A. Biological activity of 6-pentyl-2*H*-pyran-2-one and its analogs. *J. Agric. Food Chem.* **1997**, *45*, 2774−2776.

(21) Vinale, F.; Sivasithamparam, K.; Ghisalberti, E. L.; Marra, R.; Barbetti, M. J.; Li, H.; Woo, S. L.; Lorito, M. A novel role for *Trichoderma* secondary metabolites in the interactions with plants. *Physiol. Mol. Plant Pathol.* **2008**, *72*, 80−86.

(22) Vinale, F.; Flematti, G.; Sivasithamparam, K.; Lorito, M.; Marra, R.; Skelton, B. W.; Ghisalberti, E. L. *Harzianic acid*, an antifungal and plant growth promoting metabolite from *Trichoderma harzianum*. *J. Nat. Prod.* **2009**, *72*, 2032−2035.

(23) Vinale, F.; Sivasithamparam, K.; Ghisalberti, E. L.; Woo, S. L.; Nigro, M.; Marra, R.; Lombardi, N.; Pascale, A.; Ruocco, M.; Lanzuise, S.; Manganiello, G.; Lorito, M. *Trichoderma* secondary metabolites active on plants and fungal pathogens. *Open Mycol. J.* **2014**, *8*, 127−139.

(24) Vinale, F.; Nigro, M.; Sivasithamparam, K.; Flematti, G.; Ghisalberti, E. L.; Ruocco, M.; Varlese, R.; Marra, R.; Lanzuise, S.; Eid, A.; Woo, S. L.; Lorito, M. Harzianic acid: A novel siderophore from *Trichoderma harzianum*. *FEMS Microbiol. Lett.* **2013**, *347*, 123−129.

(25) Kruger, N. J.; Troncoso-Ponce, M. A.; Ratcliffe, R. G. ^{1}H NMR metabolite fingerprinting and metabolomic analysis of perchloric acid extracts from plant tissues. *Nat. Protoc.* **2008**, *3*, 1001−1012.

(26) Kim, H. K.; Choi, Y. H.; Verpoorte, R. NMR-based plant metabolomics: Where do we stand, where do we go? *Trends Biotechnol.* **2011**, *29*, 267−275.

(27) Mannina, L.; Sobolev, A. P.; Capitani, D. Applications of NMR metabolomics to the study of foodstuffs: Truffle, kiwifruit, lettuce, and sea bass. *Electrophoresis* **2012**, *33*, 2290−2313.

(28) Wu, X.; Li, N.; Li, H.; Tang, H. An optimized method for NMR-based plant seed metabolomic analysis with maximized polar metabolite extraction efficiency, signal-to-noise ratio, and chemical shift consistency. *Analyst* **2014**, *139*, 1769−1778.

(29) Sobolev, A. P.; Segre, A.; Lamanna, R. Proton high-field NMR study of tomato juice. *Magn. Reson. Chem.* **2003**, *41*, 237−245.

(30) Sánchez Pérez, E. M.; Iglesias, M. J.; Ortiz, F.; Sánchez Pérez, I.; Galera, M. M. Study of the suitability of HRMAS NMR for metabolic profiling of tomatoes: Application to tissue differentiation and fruit ripening. *Food Chem.* **2010**, *122*, 877−887.

(31) Hediji, H.; Djebali, W.; Cabasson, C.; Maucourt, M.; Baldet, P.; Bertrand, A.; Zoghlami, L. B.; Deborde, C.; Moing, A.; Brouquisse, R.;

DOI: 10.1021/acs.jafc.6b00801
J. Agric. Food Chem. XXXX, XXX, XXX−XXX

Chaıbi, W.; Gallusci, P. Effects of long-term cadmium exposure on growth and metabolomic profile of tomato plants. *Ecotoxicol. Environ. Saf.* **2010**, *73*, 1965−1974.
(32) López-Gresa, M. P.; Maltese, F.; Bellés, J. M.; Conejero, V.; Kim, H. K.; Choi, Y. H.; Verpoorte, R. Metabolic response of tomato leaves upon different plant−pathogen interactions. *Phytochem. Anal.* **2010**, *21*, 89−94.
(33) Iglesias, M. J.; López, J. G.; Luján, J. F. C.; Ortiz, F. L.; Pereznieto, H. B.; Toresano, F.; Camacho, F. Effect of genetic and phenotypic factors on the composition of commercial marmande type tomatoes studied through HRMAS NMR spectroscopy. *Food Chem.* **2014**, *142*, 1−11.
(34) Benard, C.; Bernillon, S.; Biais, B.; Osorio, S.; Maucourt, M.; Ballias, P.; Deborde, C.; Colombié, S.; Cabasson, C.; Jacob, D.; Vercambre, G.; Gautier, H.; Rolin, D.; Genard, M.; Fernie, A. R.; Gibon, Y.; Moing, A. Metabolomic profiling in tomato reveals diel compositional changes in fruit affected by source−sink relationships. *J. Exp. Bot.* **2015**, *66*, 3391−3404.
(35) Doty, F. D.; Entzminger, G.; Yang, A. Y. Magnetism in high-resolution NMR probe design. II: HR MAS. *Concepts Magn. Reson.* **1998**, *10*, 239−260.
(36) Mazzei, P.; Piccolo, A. ^{1}H HRMAS-NMR metabolomic to assess quality and traceability of mozzarella cheese from Campania buffalo milk. *Food Chem.* **2012**, *132*, 1620−1627.
(37) Mazzei, P.; Piccolo, A.; Nugnes, L.; Mascolo, M.; De Rosa, G.; Staibano, S. Metabolic profile of uterine leiomyomas intact tissue using high resolution magic-angle spinning ^{1}H NMR spectroscopy. *NMR Biomed.* **2010**, *23*, 1137−1145.
(38) Brereton, R. G. Pattern recognition. Data analysis for the laboratory and chemical plant. In *Chemometrics*; Eilers, P., Ed.; John Wiley & Sons: Chichester, U.K., 2003; Chapter 4, pp 183−269, DOI: 10.1002/0470863242.ch4.
(39) Worley, B.; Powers, R. Multivariate analysis in metabolomics. *Curr. Metabolomics* **2012**, *1*, 92−107.
(40) Mazzei, P.; Piccolo, A. Interactions between natural organic matter and organic pollutants as revealed by NMR spectroscopy. *Magn. Reson. Chem.* **2015**, *53*, 667−678.
(41) Ceoldo, S.; Toffali, K.; Mantovani, S.; Baldan, G.; Levi, M.; Guzzo, F. Metabolomics of *Daucus carota* cultured cell lines under stressing conditions reveals interactions between phenolic compounds. *Plant Sci.* **2009**, *176*, 553−565.
(42) Sung, J.; Lee, S.; Lee, Y.; Ha, S.; Song, B.; Kim, T.; Waters, B. M.; Krishnan, H. B. Metabolomic profiling from leaves and roots of tomato (*Solanum lycopersicum L.*) plants grown under nitrogen, phosphorus or potassium-deficient condition. *Plant Sci.* **2015**, *241*, 55−64.
(43) Wojtaszek, P. *Neurotransmitters in Plant Life*; Roschina, V. V.; Ed.; Science Publishers, Inc.: Enfield, NH, 2001.
(44) Di Sansebastiano, G. P.; Fornaciari, S.; Barozzi, F.; Piro, G.; Arru, L. New insights on plant cell elongation: A Role for Acetylcholine. *Int. J. Mol. Sci.* **2014**, *15*, 4565−4582.
(45) Akihiro, T.; Koike, S.; Tani, R.; Tominaga, T. S.; Watanabe, T.; Iijima, Y.; Aoki, K.; Shibata, D.; Ashihara, H.; Matsukura, C.; Akama, K.; Fujimura, T.; Ezura, H. Biochemical mechanism on GABA accumulation during fruit development in tomato. *Plant Cell Physiol.* **2008**, *49*, 1378−1389.
(46) Chardon, F.; Bedu, M.; Calenge, F.; Klemens, P. A. W.; Spinner, L.; Clement, G.; Chietera, G.; Léran, S.; Ferrand, M.; Lacombe, B.; Loudet, O.; Dinant, S.; Bellini, C.; Neuhaus, H. E.; Daniel-Vedele, F.; Krapp, A. Leaf fructose content is controlled by the vacuolar transporter SWEET17 in *Arabidopsis*. *Curr. Biol.* **2013**, *23*, 697−702.
(47) Chiang, P. K.; Gordon, R. K.; Tal, J.; Zeng, G. C.; Doctor, B. P.; Pardhasaradhi, K.; McCann, P. P. *S*-Adenosylmethionine and methylation. *FASEB J.* **1996**, *10*, 471−480.
(48) Winkel-Shirley, B. Biosynthesis of flavonoids and effects of stress. *Curr. Opin. Plant Biol.* **2002**, *5*, 218−223.
(49) Corea, O. R. A.; Bedgar, D. L.; Davin, L. B.; Lewis, N. G. The arogenate dehydratase gene family: Towards understanding differential regulation of carbon flux through phenylalanine into primary versus secondary metabolic pathways. *Phytochemistry* **2012**, *82*, 22−37.
(50) Minorsky, P. V. Trigonelline: A diverse regulator in plants. *Plant Physiol.* **2002**, *128*, 7−8.

DOI: 10.1021/acs.jafc.6b00801
J. Agric. Food Chem. XXXX, XXX, XXX−XXX